Mining, Metallurgy & Exploration (2024) 41:695–705
https://doi.org/10.1007/s42461-024-00925-3

Contribution of Individual Support Components to Roof Stability in a Longwall Gateroad

Zoheir Khademian[1] · **Morgan Sears**[1]

Received: 25 July 2023 / Accepted: 19 January 2024 / Published online: 13 February 2024

Abstract
According to the 2010–2019 Mine Safety and Health Administration (MSHA) accident report database, 91% of reported ground control accidents in US longwall mines were caused by roof instability. Gateroads are subjected to significant changes in loading conditions from the development to the longwall abutment loading phases. When combined with thinly bedded shale roof, found in many US longwall coal mines, the design of efficient roof support becomes challenging. In previous work, the bonded block modeling (BBM) of roof by UDEC was validated against field extensometer measurements in a longwall entry roof at a 180-m depth of cover. The BBM was shown capable of capturing delamination and buckling of shale roof, one of the main roof instability mechanisms in longwall mines. This paper presents the recent findings on the roof-support interaction using BBM models of the same longwall entry. The effects of cable bolts, roof bolt density, and strap support on potential roof instability are studied. Results demonstrate the potential for BBM numerical models to help understand the complex roof and support system interactions and to assist with optimizing gateroad support systems.

Keywords Entry roof stability · Roof-support interaction · Bonded block models · Trigons · Longwall mine

1 Introduction

The design of support systems for gateroad entries in US longwall mines is mostly through local experience and in-mine trial and error that may lead to under-designed or over-designed support patterns. MSHA database shows that from 2010 to 2019, roof falls accounted for 91% of total reported ground control accidents in the US underground coal mines [15]. One of the challenges in developing support design guidelines for entry roof in longwall mines is the variation of support performance with roof geology and stress patterns. The contribution of individual support elements is difficult to quantify in an operating mine because the support system is required to be fully functional at all times and removing certain supports to assess their contribution to stability is not prudent. In addition, local changes in the geology complicate the evaluation of the results of field trails. The National Institute for Occupational Safety and Health (NIOSH) has initiated a research project to evaluate methods for designing entry roof supports by collecting data on the roof geology and support systems in US longwall mines, conducting field instrumentations and laboratory testing, and developing numerical models.

Numerical models validated against field data can be useful tools to examine the support performance under different geologic and stress conditions. However, the performance of conventional continuum modeling tools is inherently limited when the rock failure mechanism is mostly delamination and buckling of rock strata [21] and [4], two main mechanisms governing roof instability in US longwall mines [9]. Esterhuizen et al. [5] used a combined brittle/shear mechanism and realistically simulated the strength anisotropy and delamination of bedded strata in continuum models. However, discontinuous (discrete) modeling techniques known as discrete element method (DEM) [2] implemented in universal distinct element code (UDEC) [10] or hybrid continuous-discontinuous techniques such as FDEM [14] implemented in IRAZU software (Geomechanica Inc. [8]) are expected to be more effectively represent the mechanical response of rock and its interaction with the support systems. This is because discontinuous or hybrid techniques allow for fracture initiation and propagation in rock as they treat the rock as an assembly of separate blocks that can slide, rotate, and even

✉ Zoheir Khademian
opv9@cdc.gov

[1] Pittsburgh Mining Research Division, CDC NIOSH, Pittsburgh, PA, USA

detach if dominant stress exceeds their overall strengths. The classic formulation of UDEC did not allow fracture propagation within an intact rock, but Lorig and Cundall [12] showed that a bonded block pattern such as Voronoi tessellation can overcome the shortcoming. Figure 1 is the concept behind the bonded block modeling that has recently found wide applications in rock mechanics [17], 18. As shown in Fig. 1, a discontinuity in BBM is initiated and propagated when the stress level at the interface between bonded blocks exceeds thresholds either in shear or in tension.

While the majority of previous studies using BBM have focused on the laboratory-scale rock fracturing process, there has been some work on field-scale behavior of rock using BBM, such as modeling shear fracture propagation above coal mine entries [1], the longwall caving process [7], and coal rib spalling [16]. For validating the BBM technique for studying longwall entry roof response, Khademian et al. [11] evaluated the BBM technique using the UDEC. The authors constructed an entry-scale model of a longwall mine in West Virginia and validated the BBM modeling results against field measurements. This paper presents further work to evaluate the contribution of different support units to the stability of the entries using the validated BBM models. This series of studies aims to develop procedures for modeling supported entries and the surrounding rock mass. In the next step, the developed modeling procedures will further be used to develop a roof support design evaluation tool by generating a wide range of entry-scale models with different stress and geology conditions.

2 Modeling Methodology

The BBM technique in UDEC is used to model rock as an assembly of smaller blocks with triangular shapes (trigon), bonded together at their contacts with cohesion and tensile strengths (Fig. 1). The so-called micromechanical properties associated with trigons are the contacts' normal and shear stiffnesses, cohesion, and tensile strengths that together with the block material properties determine the macromechanical response of the assembled rock unit. The blocks themselves were treated as elastic materials. A longwall mine in West Virginia was selected for evaluating support performance by the BBM technique. A detailed-scale model of the gateroad entry in the study mine was constructed, and the micromechanical properties assigned to the trigon blocks were discussed previously [11]. The boundary conditions on the entry model after the development phase were obtained from field monitoring and panel-scale numerical modeling results in the study mine [5]. The entry development was modeled by removing materials within the boundaries of the entry and then gradually releasing traction on the mined boundaries in ten decremental loading steps. The primary and secondary support system components were installed at the seventh step in the unloading process, assuming the 10th unloading step represents the completion of the entry development phase.

The abutment loading was extracted from the panel-scale model above the roof line at the corner of the tailgate entry. Then, the loading was applied to the boundary of the entry model in stages. The vertical loads were applied directly to the top of the model. The horizontal loading was gradually applied to the side of the model for each stage of mining using a displacement-controlled loading until the desired stress conditions were met at a location 3 m above the roof line. The modeled roof was considered failed when the roof slabs were accelerating (increasing velocity) under constant boundary loading conditions. Khademian et al. [11] used this approach and showed that the displacement of different units in the roof after support installation is close to the extensometer measurements conducted in a study site.

3 Description of Mine Site

The research takes place in a longwall mine in West Virginia, mining the lower Kittanning coal bed with 152 to 243 m of cover. The width of the longwall panels is 365 m.

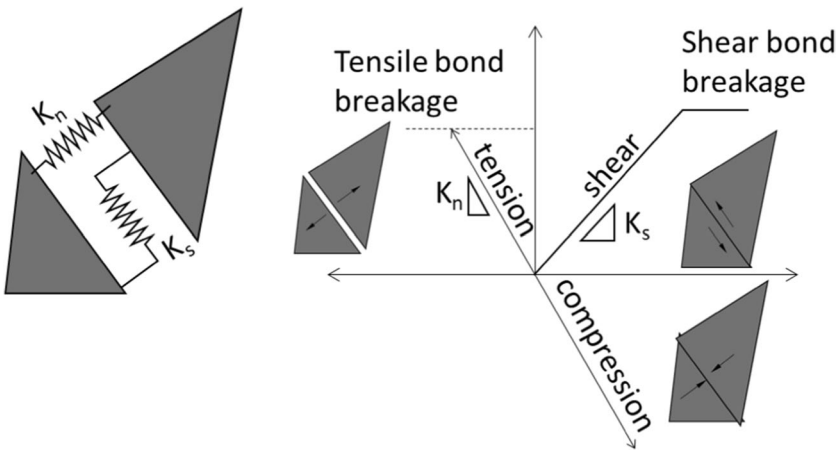

Fig. 1 UDEC modeling of fracture propagation in a medium assembled by triangular blocks (trigon)

The mining height is about 2.1 m with the entry development height up to 2.4 m. The width of the entry and crosscut developments is 5.5 m. The instrumentation site is in the tailgate of the third panel in the district under 180 m of cover and was part of a three-entry gateroad system as shown in Fig. 2. Overcore stress measurements were conducted at the instrumentation site. The major horizontal stress was measured 1100 psi with N80W orientation. The minor horizontal stress was measured 850 psi. The main development directions of the mine are oriented at about 45° to the major horizontal stress, and thus the tailgate is exposed to unfavorable horizontal stress concentrations.

Instrumentation and then monitoring were started a few days after the development of the gateroad entries and continued until the second panel mine-by. Figure 2 shows the details of the mine layout and location of the instrumentation site on the last day of monitoring.

3.1 Geotechnical Setting and Instrumentation Site

The overburden in the study mine consists of alternating sandstone and shale beds with sandstone layers between 9 and 18 m thick. The thinly bedded shale above the Lower Kittanning coalbed ranges from dark gray to carbonaceous clay shale. The Johnstown limestone is located above this sandy zone. Table 1 lists the strength and mechanical properties of the rocks within the immediate roof. As shown by Esterhuizen et al. [6], the Coal Mine Roof Rating (CMRR) [13] is used to estimate the large-scale field strength of the strata.

The support performance was measured by load cells installed underneath the face plates of the cable bolts at the time of installation. The cable bolt load cells and roof extensometer were installed between 20 and 30 m outby the advancing heading. The roof sag was monitored by three 2.4-m-long extensometers (No. 1, No. 2, and No. 3 in Fig. 5a) and one roof extensometer of 6 m length (No. 5 in Fig. 5a).

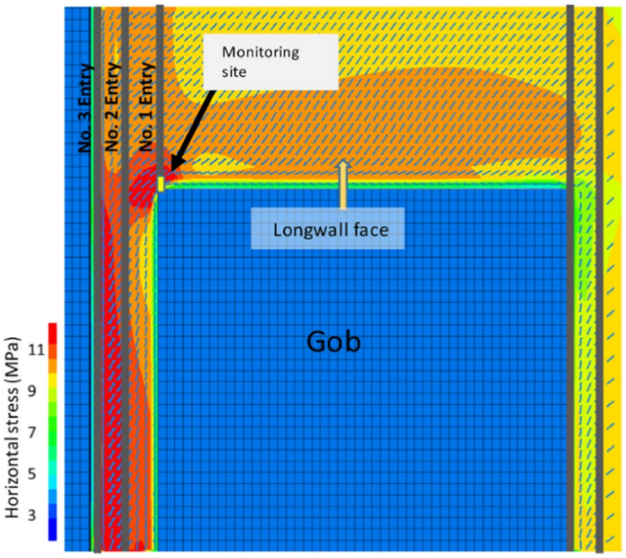

Fig. 3 Maximum horizontal stress distribution and orientation 3 m above the mined coal bed in the panel-scale model in FLAC3D. Details of the model can be found in Esterhuizen et al. [5]. This model was used to obtain stress paths for the UDEC entry-scale model

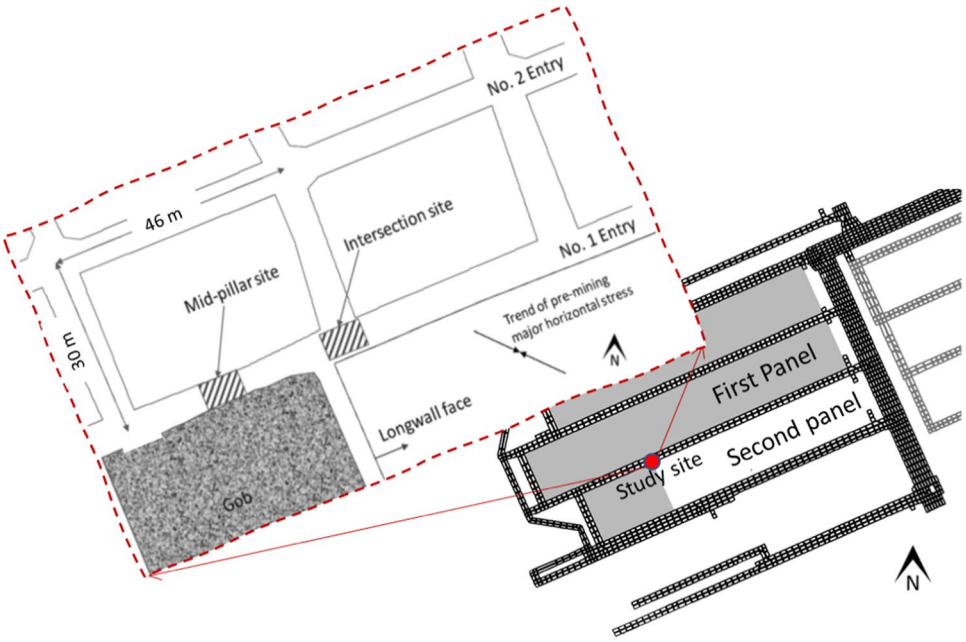

Fig. 2 Pillar layout and monitoring site location at the longwall mine selected for this study

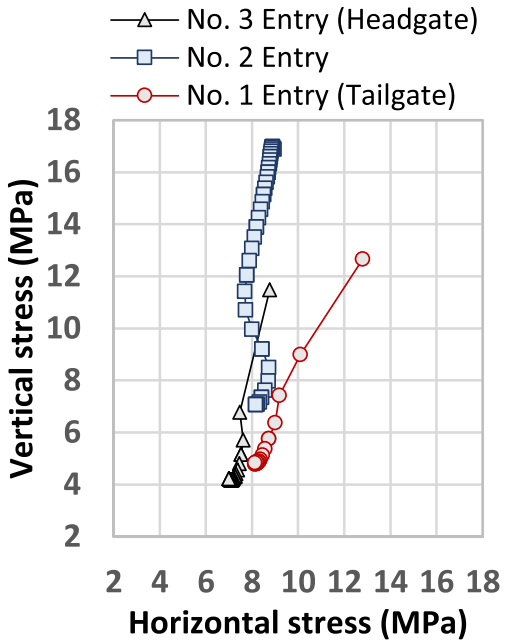

Fig. 4 Stress paths experienced by three entries in the FLAC3D model in a vertical plane perpendicular to the long axis of the entry. The detail of the FLAC3D model can be found in Esterhuizen et al. [5]

3.2 Support System

The primary roof support in the study mine was rows of four fully grouted #6 bars with a 1.8 m height, spaced on 1.2-m centers. Fully grouted bolts were also installed at a 45° angle at the corner of the rib and roof, spaced on 2.4-m centers. The secondary support of the roof was a pair of cable bolts (3 m by 15 mm) installed through a strap every 2.4 m with 1.2 m of resin grout. Secondary support was installed about 18.2 to 30.4 m outby the advancing face. The standing support system was also used in the form of two rows of nine-point wooden cribs, but they are not considered in the models here because from crib load measuring devices, the standing supports did not take noticeable loads until after the second panel mined by.

4 Numerical Modeling

In order to model thinly bedded rock units, trigons in the scale of centimeters should be constructed. For full-scale modeling of longwall mines, this level of detail leads to prohibitive computation time. One approach is to use sub-modeling where stress boundary conditions for an isolated area are obtained from a low-resolution (panel-scale) model and then are used to define the boundary conditions in a high-resolution (entry-scale) model as described in the following sections.

4.1 Entry Loading Condition by Panel-Scale Model

Tulu et al. [20] constructed a panel-scale model of the study site and validated the stress variation during mining against field measurements by Hollow Inclusion (HI) stress cells. The stress around the gateroad entries in the model was used here to define the boundary condition of the entry-scale models. Stress distribution results from the panel-scale models at the end of the monitoring period with the actual longwall panel layout are shown in Fig. 3.

Figure 4 shows the gateroad loading paths from the model recorded as the vertical and horizontal stresses at different mining stages, recorded 3 m above the roof line. In Fig. 4, each marker on the curves shows a 9-m advance of the longwall face. The initial stress state in the model is with the horizontal stress of 7.1 MPa and vertical stress of 4.2 MPa. Compared to the other two entries, the stress path of the No. 1 (tailgate) entry shows a higher increase in horizontal

Table 1 Key field-scale rock properties at the study site

Rock type	Elastic modulus (GPa)	Friction angle (degrees)	Cohesion (MPa)	Tensile strength (MPa)
Limestone	50	30	34	11
Gray clay shale	8	28	6	2
Clay shale	10	28	7	2
Carbonaceous shale	15	28	11	4
Shaley sandstone	18	38	10	3
Black shale	7.5	28	5.2	1.7
Claystone (calcareous)	15	28	10.4	3.4
Dark gray shale	15	28	10.4	3.5
Dark gray claystone	7.5	28	5.2	1.7
Gray silty shale	13.8	28	9.6	3.2
Dark gray shale with coal streaks	8.8	28	6	2

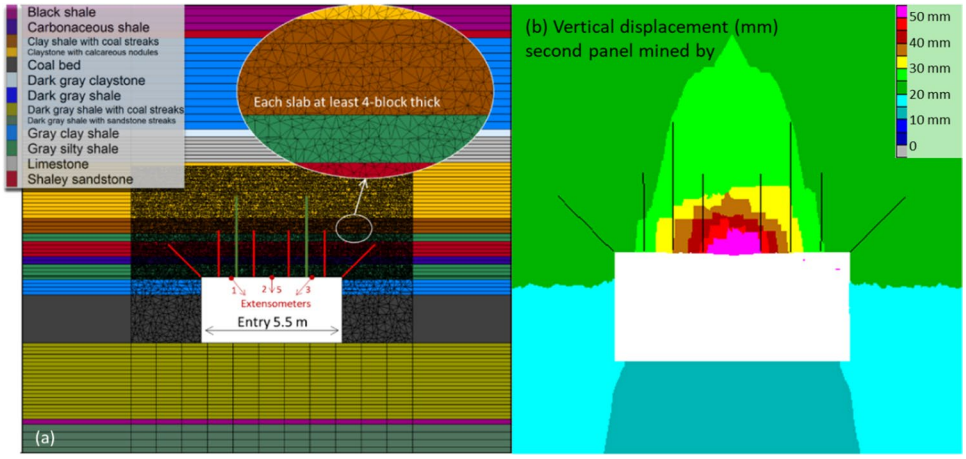

Fig. 5 **a** Lithology profile of the roof and floor at the monitoring site along with the support system and also trigons' geometry and density. **b** Model results for vertical displacement after second panel mine-by [11]

stress. After the second panel mines by the monitoring site, stress at this location in the model reaches 12.8 and 12.7 MPa in horizontal and vertical directions, respectively. The change in stresses recorded by HI stress cells showed that 8 m above the tailgate roof, the vertical and horizontal stress values were 10.3 MPa and 11.5 MPa, respectively. With this validation, the stress path obtained from the model (Fig. 4) at the tailgate entry (entry No. 1) is applied as the boundary conditions of BBM entry-scale models described in the following section.

4.2 Entry-Scale Model of the Site

Figure 5a shows the entry-scale model constructed for the study site, which is a two dimensional or a vertical slice through entry No. 1. In total, 92 bedding planes in the roof and floor are modeled. Up to 11.5 m above the roof line, 65 slabs each 10 to 20 cm thick are modeled. BBM trigon blocks were generated up to 5 m above the roof line, and the rest of the thinly bedded strata were modeled with no trigons.

The edge of trigons varies from 0.02 to 0.06 m according to the thickness of each slab so that at least four trigons are located across each slab. The mine did not install rib bolts except at the pillar corners, indicating that rib spalling was not a concern during the longwall retreat. Thus, 3 m of ribs are constructed with relatively large trigons of 0.2 m edge to reduce computation time.

The modeling results from previous work are shown in Fig. 5b, as the roof vertical displacement after the second panel is mined by the instrumentation site. Figure 6a shows the roof vertical displacements at the left-hand and right-hand sides of the entry roof, confirming that the values predicted by the model are in agreement with the extensometer readings at the site. Figure 6b confirms the agreement between model and field measurements of the vertical

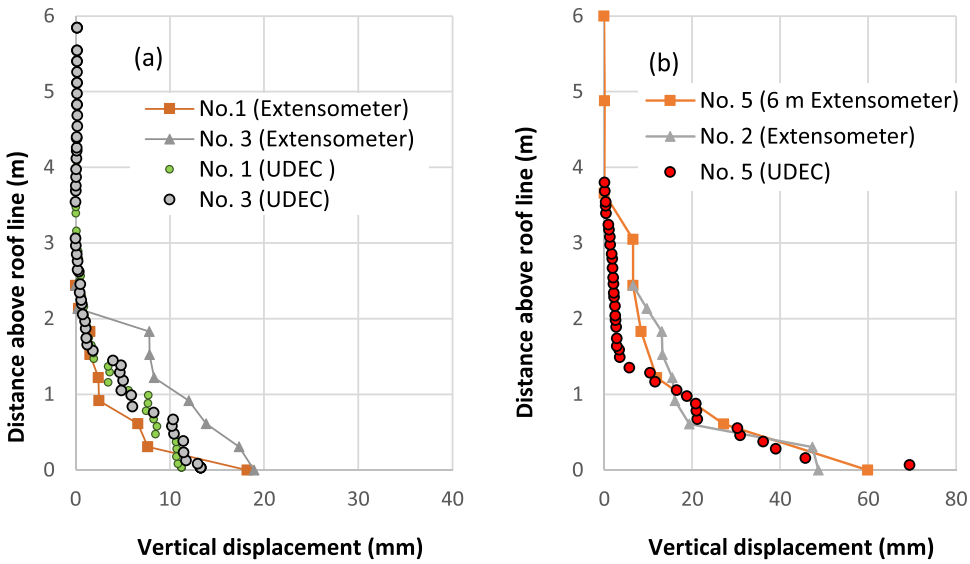

Fig. 6 Vertical displacement above the roof line from model and field extensometers at **a** the No. 1 and No. 3 extensometer locations and **b** No. 2 and No. 5 extensometer locations shown in Fig. 4 [11]

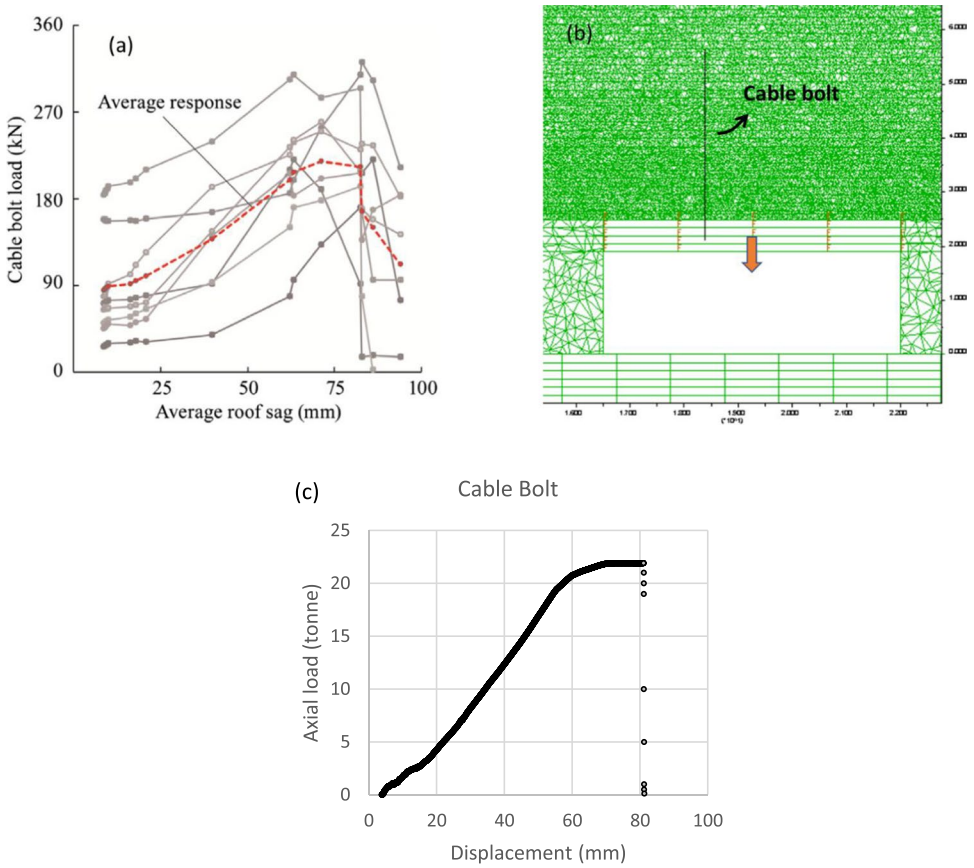

Fig. 7 Cable bolts response measure in the field and respective model calibration. **a** Load cell results in 8 cable bolts instrumented in the field. **b** Model geometry for calibrating bolt mechanical parameters. **c** Calibrated cable bolt response

displacements at the center of the roof. The validated model is considered Case A and is used to study support system alternatives under similar conditions.

5 Support Alternatives

In this part, models with different support components are studied. Before evaluating different support alternatives, some detail is provided for numerical calibration of the fully grouted and cable bolts that are installed in the models.

5.1 Calibration

The cable bolt response under mining-induced stresses is calibrated against the field measurements. Figure 7a shows the response of 8 cable bolts measured by the load cells versus the average roof sag measured by the extensometers. Most of the cable bolts were loaded between 50 to 100 kN when monitoring started, which was a few days after the bolt installation. This initial load can be associated with the thrust of the bolt machine during installation, and the displacement occurred after the installation. The peak load of individual bolts ranged from 190 to 320 kN with an average of 245 kN, which is close to the expected pick strength. The peak load for the cable bolts occurred between 60 to 90 mm of the roof sag. The average stiffness of the cable bolts from the slope of the curve between 16 and 70 mm of roof sag was 2.3 kN/mm, lower than the typical stiffness value measured during a controlled testing setup [19].

In an effort to calibrate the cable bolts under in situ modeling conditions, the model in Fig. 7b is used to conduct a

Table 2 Mechanical properties of the fully grouted bolts and cable bolts

Type	Mechanical properties				
	Tensile yield force (kN)	Out-of-plane spacing (m)	Young's modulus (GPa)	Grout shear stiffness (kN/m/m)	Grout shear strength (kN/m)
Cable bolt	260	2.4	30.5	18,000	250
Fully grouted bolt	190	1.2	200	18,000	250

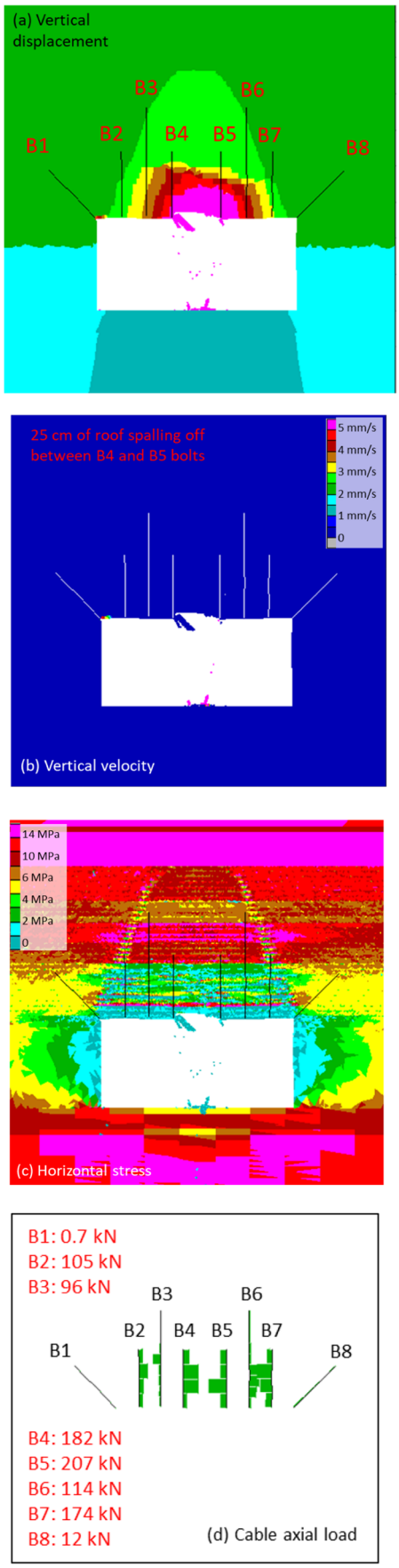

Fig. 8 Model results showing entry response for Case #2 support system, assessing effects of the strap. **a** Vertical displacement (m), **b** vertical velocity (m/s), **c** horizontal stress (pa), **d** bolt axial load (kN) ▶

pullout test on one of the cable bolts in the roof. The bolt head is extended to include a block hanging from the roof with a thickness of 0.5 m. The block is pulled downwards, and the load in the bolt is recorded versus the block displacement downwards. Through a trial-and-error approach, the cable and grout parameters are calibrated to match the average response of the cable bolts in Fig. 7a. Figure 7c shows the force–displacement curve of the cable bolt response after calibration. Table 2 lists the calibrated mechanical properties used for modeling the bolts.

One aspect of using a 2D software program to model a 3D environment is the scaling of support properties to account for the support spacing in the third dimension. Donovan et al. [3] showed that linear scaling of material properties is effective in applying effects of regularly spaced patterns in a 3D system on the behavior of materials in 2D environments. For considering the spacing of fully grouted bolts (1.2 m) and cable bolts (2.4 m) along the entry, we scale their mechanical properties. Thus, the elastic modulus and tensile strength of the cables and bolts and the stiffness and cohesion strength of the grout are divided by their spacing along the entry.

Besides the support systems installed in the mine with model results presented above, the effects of different support components on the roof are evaluated through studying four additional cases. Case #2 looks at the support performance without the strap through which cable bolts were installed. Case #3 removes the 45-degree bolts from the support system. In addition to the 45-degree bolts, Case #4 removes the cable bolts and shows the major effects of cable bolts. Finally, Case #5 evaluates the roof response when the support is reduced by 0.3 m (1 ft) to 1.5-m-long bolts across the entry.

5.2 Case #2: Effects of Strap Support

As the first step, the effects of strap support on the roof stability are studied by removing the strap through which cable bolts are installed in the mine. The model is run according to the procedure in the modeling methodology section and is loaded through the full abutment loading sequence. Results of the model are shown in Fig. 8a–d. Figure 8a shows the vertical displacement profile of the roof, showing that without the strap support, the roof layers became fragmented between bolts and the three first shale slabs (failure depth of 25 cm) spalled off between fully grouted bolts No. 4 and 5. However, the roof remains stable as shown by the velocity plot in Fig. 8b where the roof velocity remained close to zero after the second panel mine-by. The horizontal stress

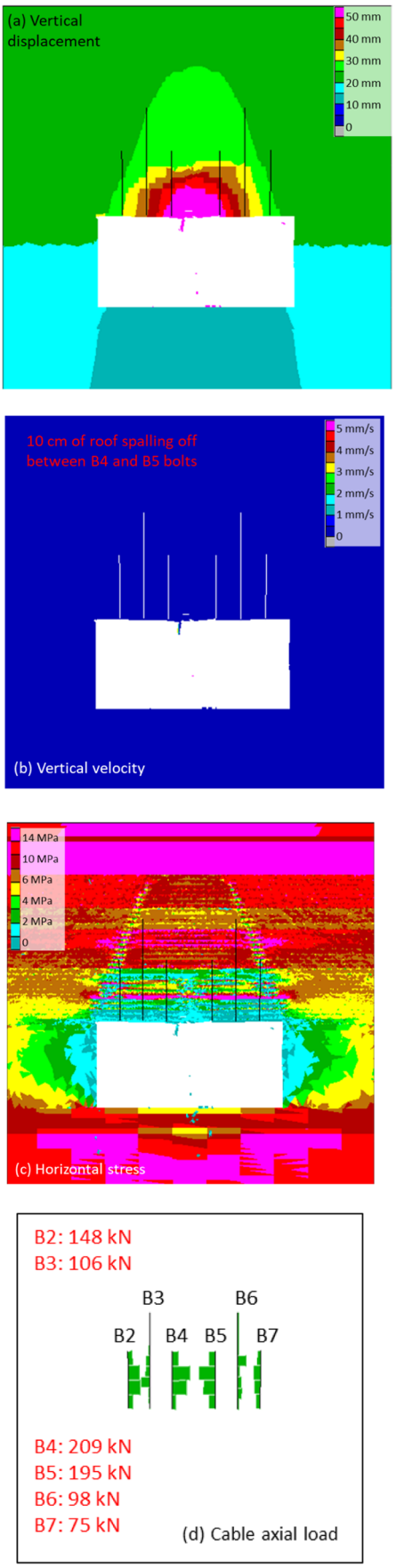

Fig. 9 Model results showing entry response for Case #3 support system, assessing effects of 45-degree bolts. **a** Vertical displacement (m), **b** vertical velocity (m/s), **c** horizontal stress (pa), **d** bolt axial load (kN)

profile shown in Fig. 8c indicates the transfer of loads to the relatively stronger shale layer, 40–50 cm above the roof line. Figure 8d shows the maximum load in each of the bolts numbered from 1 to 8. Except for the B1 and B8 bolts that took minimal loads, the rest of the bolts have surpassed their yield strengths. The straps are demonstrated to provide local support to the immediate roof between the bolts, preventing the potential for injury by smaller rock fragments.

5.3 Case #3: Effects of 45-Degree Bolts

From Case #2 observation, straps were shown to be useful for controlling local roof falls between bolts at the center of the entry. Also, it was shown that the 45-degree bolts (B1 and B8) seem to have little role in the roof control. To further evaluate B1 and B8 bolt performance, in Case #3, the model run is repeated without installing these two bolts. The results are shown in Fig. 9a–d. From Fig. 9a, the local roof spalling is limited to 10 cm above the roof line, but the overall displacement profile remains the same as that in Fig. 8a. The roof remains stable as shown in Fig. 9b. The horizontal stress is transferred to a stronger rock unit 60 to 80 cm above the roof line, 20 to 30 cm higher than that in the case with B1 and B8 bolts installed. From Fig. 9d, the loads in the bolts stay similar to Case #2, showing that installing B1 and B8 bolts appears to have no significant effects on the roof stability. In fact, the lack of bolts B1 and B8 leads to the transfer of load higher in the roof with less skin damage. The B1 and B8 bolts are no longer installed at the case study mine after conducting an in-mine experiment prior to this study being conducted.

5.4 Case #4: Effects of Cable Bolts

In Case #4, the performance of cable bolts is evaluated by removing them from the support system and repeating the model runs. The results are shown in Fig. 10a–d. In Fig. 10a, the roof is shown to be unstable. The velocity plots in Fig. 10b show that 60 cm of the roof will collapse. Loads are transferred to the layers above 90 cm in the roof but are mainly concentrated in 1.6 m above the roof in the strong shaley sandstone unit (Fig. 10c). Segments of the bolts that are not broken yet take considerable load mainly because their last segment is 25 cm in the strong shaley sandstone, transferring the loads to the upper layers. Thus, in the next

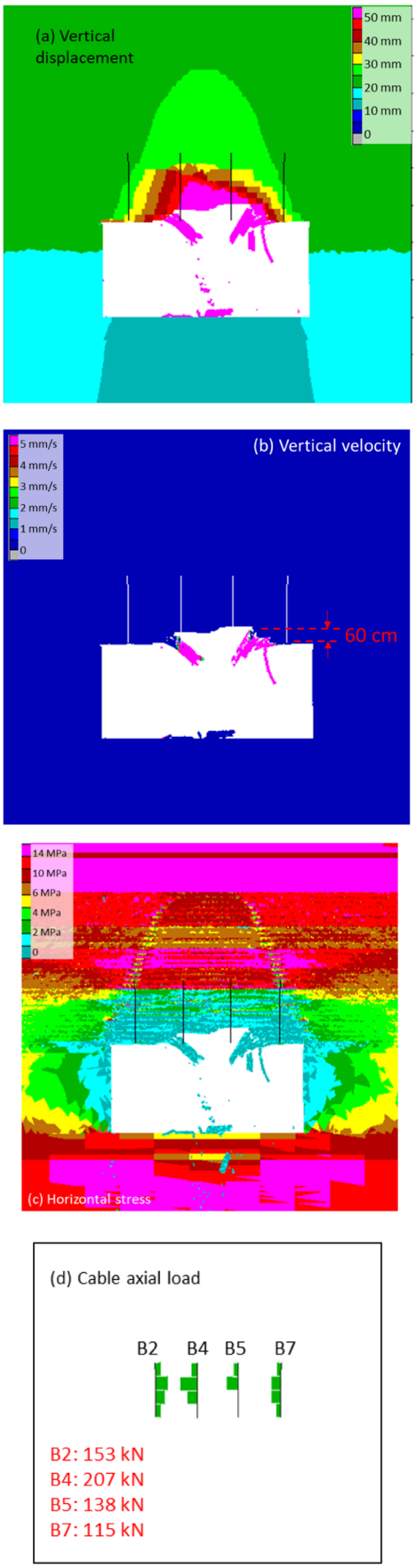

Fig. 10 Modeling results for support system Case #3 for 6-ft long fully grouted bolts with no 45-degree bolts and no cable bolts. **a** Vertical displacement (m), **b** vertical velocity (m/s), **c** horizontal stress (pa), **d** bolt axial load (kN)

case, the length of the bolts is reduced so they are not within the strong shaley sand.

5.5 Case #5: Effects of Primary Bolts

In the last step of the support performance evaluation, a minimal support layout is modeled by installing four fully grouted bolts with 1.5 m length (5 ft) evenly spaced across the entry. The difference with Case #4 is the reduction in the length of the primary bolts by 0.3 m (1 ft). The results are shown in Fig. 11a–d.

Figure 11a shows significant roof movement up to 1.6 m above the roofline where the strong shaley sandstone unit is located. Figure 11b confirms the total collapse of the roof up to this depth. Figure 11c shows that the horizontal stress is close to zero and loads are transferred to the layer 1.6 m above the roof.

The results in Figs. 10 and 11 illustrate under-designed support systems that may lead to roof fall with a height of 0.6 and 1.6 m, respectively. The results demonstrate that the models agree with the judgement of the mine staff that four bolts are needed to provide adequate roof control for the longwall abutment loads and geologic conditions at the mine.

6 Discussion and Limitations

In the previous work [11] in this series of papers, the application of BBM in evaluating the stability and failure mechanism of roof in longwall entries was evaluated. It was shown that the roof deformation predicted by the model agrees with the roof extensometer recordings in an instrumentation site in a longwall mine in West Virginia. In this work, we took one step further and evaluated the performance of alternative design layout and the roles of each component through a series of parametric tests. The results showed that cable bolts prevent the collapse of 0.6 m of roof. Changing the layout to rows of 1.5-m-long primary bolts leads to the collapse of roof with a height of 1.6 m. In contrast, the fully grouted 45-degree bolts appeared to have no significant effects for controlling the roof although might be useful for controlling cutters. Straps were shown to be effective in supporting 10 to 25 cm of the roof between the fully grouted primary bolts. However, the conclusions drawn here are based on

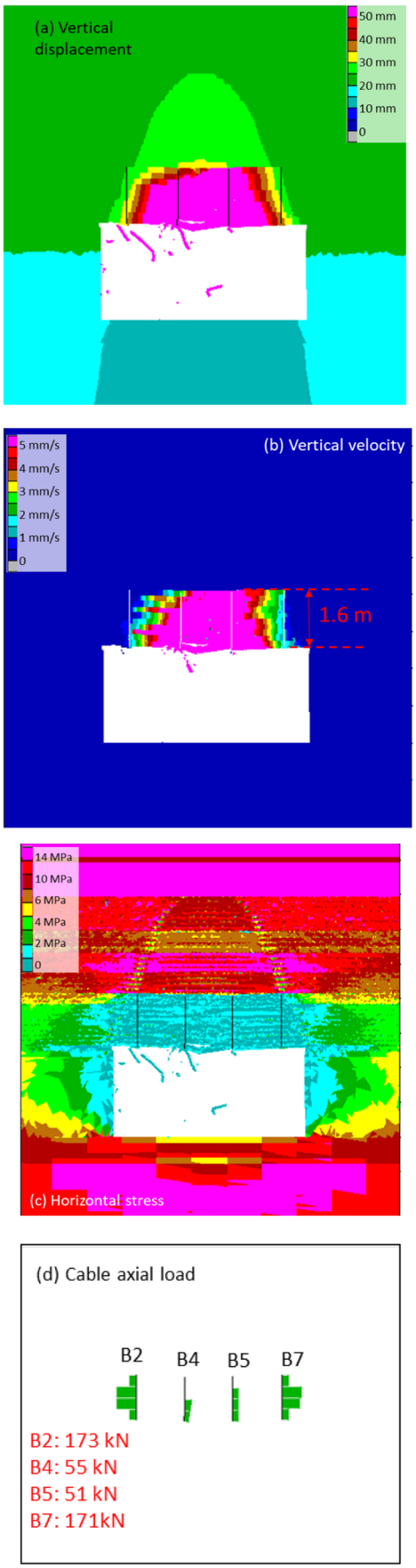

Fig. 11 Modeling results for support system Case #4 for 5-ft long fully grouted bolts with no 45-degree bolts and no cable bolts. **a** Vertical displacement (m), **b** vertical velocity (m/s), **c** horizontal stress (pa), **d** bolt axial load (kN)

the geology of the presented case and the dominant stress conditions and may not be applicable to different geology, mine layout, and stress environments.

The application of boundary loads (Fig. 4) to the entry-scale model (Fig. 5b) from the global, panel-scale model (Fig. 3) may need further improvements. Currently, vertical loads are applied as a single loading step for each stage of mining, according to Fig. 4, while the horizontal stresses are applied using velocity-controlled loading in a gradual manner. The dynamic effects stemmed from the loading process should be minimized by a scheme that allows gradual application of vertical and horizontal loads. This improvement may affect the roof sagging and failure mechanism while changing the support response under quasi-static conditions. Another aspect that needs further work is the scaling of roof support properties for a 2D model. As explained in Section 5.1, a linear scaling is used here, but to confirm the validity of this assumption, a 3D model is required to investigate the roof-support interaction and to make a comparison with the 2D model results.

7 Conclusion

The National Institute for Occupational Safety and Health (NIOSH) has initiated a research effort to develop an entry roof support design tool by collecting data on the roof geology and support systems in US longwall mines and conducting field instrumentations, laboratory testing, and numerical modeling. As a part of this effort, the bonded block method (BBM) is being evaluated as a modeling tool to study and understand the roof failure mechanism and its interaction with alternative support systems. In this paper, a previously constructed and validated BBM model was used to study the effects of support system components in roof stability. Results show that the 45-degree fully grouted primary bolts have little to no effects on the stability of the roof. Models of support systems without straps showed 10–25 cm of local roof fall between primary bolts. Models with no cable bolts were shown 0.6 to 1.6 m of roof failure heights. These results will pave the way for further analyses on roof support performance under different roof geology and stress conditions.

Acknowledgements The authors would like to acknowledge the contribution of Dr. Essie Esterhuizen in the development of the modeling methodology and collection of field geomechanical data.

Declarations

Conflict of Interest The authors declare no competing interests.

Disclaimer The findings and conclusions in this report are those of the author(s) and do not necessarily represent the official position of the National Institute for Occupational Safety and Health, Centers for Disease Control and Prevention.

References

1. Coggan J, Gao F, Stead D, Elmo D (2012) Numerical modelling of the effects of weak immediate roof lithology on coal mine roadway stability. Int J Coal Geol 2012(90):100–109
2. Cundall P, Hart R (1992) Numerical modelling of discontinua. Eng Comput 9(2):101–113. https://doi.org/10.1108/eb023851
3. Donovan K, Pariseau WE, Cepak M (1984) Finite element approach to cable bolting in steeply dipping VCR stopes. In: Geomechanics applications in underground hardrock mining. Society of Mining Engineers, New York, pp. 65–90
4. Esterhuizen GS (2012) A stability factor for supported mine entries based on numerical model analysis. The 31st international conference on ground control in mining. West Virginia University, Morgantown, WV
5. Esterhuizen GS, Gearhart D, Klemetti T, Dougherty H, Van Dyke M (2019) Analysis of gateroad stability at two longwall mines based on field monitoring results and numerical model analysis. Int J Min Sci Technol 29(1):35–43. https://doi.org/10.1016/j.ijmst.2018.11.021
6. Esterhuizen GS, Bajpayee TS, Ellenberger JL, Murphy MM (2013) Practical estimation of rock properties for modeling bedded coal mine strata using the Coal Mine Roof Rating. 47th US Rock Mechanics/Geomechanics Symposium. American Rock Mechanics Association, Alexandria, VA, 1634–1647
7. Gao FQ, Stead D (2014) The application of a modified Voronoi logic to brittle fracture modelling at the laboratory and field scale. Int J Rock Mech Min Sci 68:1–14. https://doi.org/10.1016/j.ijrmms.2014.02.003
8. Geomechanica Inc. (2016) IRAZU computer software. Retrieved from www.geomechanica.com
9. Hasenfus GJ, Su DWH (2006) Horizontal stress and coal mines: Twenty-five years of experience. International conference on ground control in mining. West Virginia University, Morgantown, 256–267
10. Itasca (2013) Itasca Consulting Group Inc. UDEC (Universal Distinct Element Code), Minneapolis
11. Khademian Z, Esterhuizen GS, Sears M (2022) Longwall gateroad stability analysis based on field monitoring and bonded block modeling results. In: Proceedings of the 41st international conference on ground control in mining. Canonsburg, PA
12. Lorig LJ, Cundall PA (1989, 1989) Modeling of reinforced concrete using the distinct element method. Paper presented at the Fracture of Concrete and Rock, New York, NY
13. Molinda GM, Mark C (1994) Coal Mine Roof Rating (CMRR): a practical rock mass classification for coal mines. Technical Report. NTIS issue number 199413. U.S. Department of the Interior, Bureau of Mines, Pittsburgh Research Center, Pittsburgh, PA
14. Munjiza A, Owen DRJ, Bicanic N (1995) A combined finite-discrete element method in transient dynamics of fracturing solids. Eng Comput 12(2):145–174. https://doi.org/10.1108/02644409510799532
15. Rashed G, Xue Y, Khademian Z, Sears M (2022) Ground-fall accident trends in mining: 2010 to 2019. In: Proceedings of the 41st international conference on ground control in mining. Canonsburg, PA
16. Sinha S, Walton G (2021) Modeling the behavior of a coal pillar rib using bonded block models with emphasis on ground-support interaction. Int J Rock Mech Min Sci 2021:148
17. Sinha S (2020) Advancing continuum and discontinuum models of brittle rock damage and rock-support interaction. PhD dissertation, In: Colorado school of mines. Arthur Lakes Library. https://hdl.handle.net/11124/176305
18. Stavrou A, Murphy W (2018) Quantifying the effects of scale and heterogeneity on the confined strength of micro-defected rocks. Int J Rock Mech Min Sci 102:131–143. https://doi.org/10.1016/j.ijrmms.2018.01.019
19. Tadolini CS, Tinsly J, McDonnell JP (2012) The next generation of cable bolts for improved ground control. In: Proceedings of the 31st international conference on ground control in mining. In: Proceedings of the 33rd international conference on ground control in mining. West Virginia University, Morgantown, WV, pp 27–34
20. Tulu IB, Esterhuizen GS, Gearhart D, Klemetti TM, Mohamed KM, Su DWH (2018) Analysis of global and local stress changes in a longwall gateroad. Int J Min Sci Technol 28(1):127–135. https://doi.org/10.1016/j.ijmst.2017.11.015
21. Tulu IB, Esterhuizen GS, Klemetti T, Murphy MM, Sumner J, Sloan M (2016) A case study of multi-seam coal mine entry stability analysis with strength reduction method. Int J Min Sci Technol 26(2):193–198